UDC 621.791.011

FORECASTING OF THE MECHANICAL PROPERTIES OF METAL WELDED CONNECTIONS OF PIPELINES AND TANKS, TAKING INTO ACCOUNT THE TIME PARAMETER OF WELDING

D.A. Neganov, N.A. Makhutov, A.E. Zorin,
E.P. Studenov, O.I. Kolesnikov

DOI: 10.31618/ESU.2413-9335.2022.1.98.1653

ANNOTATION

The article presents the results of experimental studies of the relationship between the welding reference variables (chemical composition of welding materials, welded elements, welding conditions), the structure formed in the welded joint, its basic mechanical properties (ductility, strength, impact toughness), and crack resistance parameters. The research consisted in carrying out standard and special tests, as well as studying the structure of the metal after heat treatment at various cooling rates. To confirm the established relationships, tests of circumferential welded joints of pipes and sheets of tanks, welded according to the technologies used in the Transneft PJSC, were carried out.

As a result, a model has been developed for predicting the mechanical properties of welded joints according to data of various levels. It was elucidated the quantitative effect of the cooling rate and structure parameters on the main mechanical properties of the welded joint. Also, empirical expressions were obtained connecting the group of mechanical properties of the metal (the ratio of the yield strength to the tensile strength, relative elongation, impact toughness), combined into a "complex coefficient of durability", and the metal crack resistance parameters used in the force criterion of fracture mechanics.

The greatest practical effect from the implementation of the developed model is achieved with the introduction of differentiated decreasing coefficients within the framework of computation for strength and durability, depending on the level of data on the welded joint used in the calculations.

Keywords: forecasting of mechanical properties, welding, circumferential welded joints, weld structure, pipeline, tank, crack resistance, load-bearing capacity

Introduction

Welded joints are one of the highly risk points in the structure of oil pipelines and tanks [1-3]. In the process of welding, the zone of the welded joint is affected by significant thermal and mechanical effects, which causes both structural changes in the metal and changes in its stress strain behavior. Ergo, forecasting the durability of welded joints becomes a much more difficult task, and their reliability naturally decreases (due to the occurrence of defects, the possibility of deviation of welding conditions from optimal values, the presence of difficult-to-predict welding stresses, etc.). First of all, this applies to mounting welded joints performed in the field, where the performance of works and their quality control are much more complicated, in comparison with factory environment.

In this regard, the improvement of methodological approaches to assessing the technical condition of welded joints of oil pipelines and tanks to determine and predict their durability is a relevant objective.

At the Transneft PJSC, the decision to repair or replace welded joints containing defects is based on the results of calculating the strength and durability of the defective zone. The calculation methods used in this case are based on both deformation criteria for reaching of limit state and force criteria of destruction.

The chosen calculation method determines the corresponding composition of special characteristics of the metal used as initial data (for example, destructive strain rate, critical stress intensity factor (SIF), etc.). Their characterization for the whole variety of steels used in the construction and repair of oil pipelines and tanks, welding technologies, welding materials, etc. is a separate and very time consuming task. At the same time, the experience of Transneft Research Institute LLC, as well as information from open sources [4] indicate the correlation of these parameters with the basic mechanical properties of the metal, which are determined by its structural state formed as a result of the imposition of a thermal welding cycle (in the case of welded joints). That is, there is a correlation shown in Figure 1.

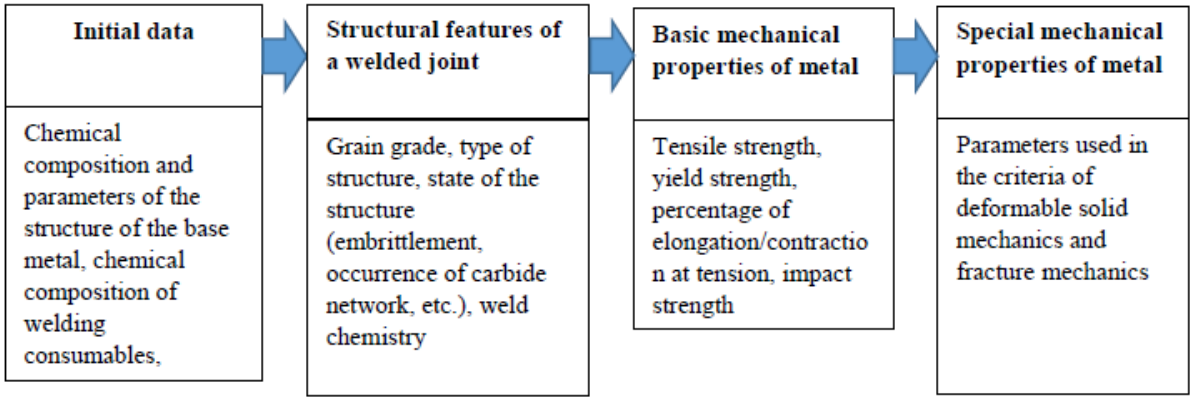

Figure 1 – The co-relation of different levels of data on the welded joint

Thus, the determination of an empirical co-relation of the blocks presented in Figure 1 will allow, in the absence of the necessary initial data, to refine them based on the available information of another level, and, at the same time, to expand the scope of the actual data on the welded joint obtained at the stage of its operation.

Experimental technique

The experimental studies performed were divided into two stages.

At the first stage, the influence of the thermal cycle of welding was being determined in the maximum possible range of cooling rates over the formed structure of the metal of the welded joint and its mechanical characteristics (including special properties used in the force criterion of fracture mechanics: critical SIF K_{Ic},, parameters of cyclic crack resistance C and n).

A pipe of strength class K56, with a diameter of 1220 mm and a wall thickness of 12.0 mm, was selected for research.

16 templates were cut from the pipe, which were then heat-treated with the parameters given in Table 1.

Table 1

Templates heat treatment parameters

No.	Heating temperature Tmax,°C	Holding time at temperature T_{max}, sec	Cooling rate in the temperature range Ac3-Ac1, °C/sec
1	1100	10	0.5
2			1.5
3			3
4			6
5			10
6			40
7			70
8			80
9	900	15	0.5
10			1.5
11			3
12			6
13			10
14			40
15			70
16			80

To perform heat treatment, a KEP 50/1250 batch-type furnace for metals was used. The cooling rate was controlled using thermocouples.

Then, samples were made from each template for metallographical observations and mechanical tests (Table 2).

Table 2

Composition of tests and studies for each heat-treated template

Item No.	Mode of test	Number of samples, pcs.	Testing technique, determinable parameters
1	Cylindrical testpiece tensile test	5	Tests in accordance with GOST 1497[1] with determination of: tensile strength σv; yield strength σt; percentage of elongation δ; - contraction ratio ψ.
2	Impact bending	5	Tests in accordance with GOST 9454[2] with the determination of impact strength KCV_{-20}
3	Cyclic crack resistance	3	Tests with determination of: number of cycles to fracture; critical SIF K_{Ic}; parameters of cyclic crack resistance C and n
4	Determination of the structural and phase composition	1	Research in accordance with GOST 5639[3], GOST 5640[4], GOST 8233[5] with determination of: content of microconstituents; grain grade

Separately, it is necessary to dwell on the test method for cyclic crack resistance. The samples, the configuration of which is shown in Figure 2, were stress-cycled with the parameters: maximum tensile rated stress in a cycle is 0.8 $\sigma_т$; the cycle asymmetry coefficient (in terms of stresses) R = 0.1; the test base is 10^5 cycles (or till destruction). Crack growth was monitored every 1000 stress cycles. For this, specially applied reference points and magnifying optical devices were used. In addition, an extensometer was installed at the place where the stress concentrator was applied. The test results were used to construct curves of crack growth rate versus stress intensity factor range (CCGR), from which the parameters *C* and *n* were determined using the method described in [5, 6], as well as the critical SIF K_{Ic} (SIF K_I at the critical crack depth) according to the expression from [7]:

$$K_I = \sigma\sqrt{\pi a}F_I(\alpha) \quad (1)$$

where σ is the nominal stress in the sample, MPa;
$\alpha = a/t$;
$F_I(\alpha) = 1{,}12 - 0{,}231\alpha + 10{,}55\alpha^2 - 21{,}72\alpha^3 + 30{,}39\alpha^4$

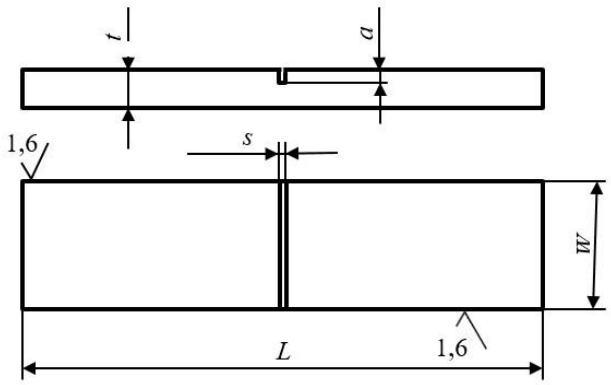

W = 20 mm; L = 200 mm; t = 11 mm; a = 0.1t; s = 0.2 mm
Figure 2 – Configuration of the test specimen for cyclic crack resistance

The values of the characteristics of the static and cyclic crack resistance of the metal (in our case, the constants K_{Ic}, *C* and *n*) may depend on the method of their preparation [8]. That is, the values of the constants determined in laboratory conditions on standard samples can differ significantly from the values characteristic of the configuration in its real operating conditions.

[1] GOST 1497-84 Metals. Tensile test methods.
[2] GOST 9454-78 Metals. Impact test method at low, room and high temperatures.
[3] GOST 5639-82 Steels and alloys. Methods for identifying and determining the size of the grain.
[4] GOST 5640-68 Steel. Metallographic method for assessing the microstructure of sheets and strips.
[5] GOST 8233-56 Steel. Microstructure standards.

Therefore, in order to confirm the universality of the results obtained within the framework of the crack resistance tests described above, model tests similar in purpose were carried out, in which both the configuration of the surface semielliptical crack and the stressed-deformed state of the pipeline under the action of internal pressure were reproduced.

To carry out model tests, four circular welded joints were made, welded by automatic welding with a solid wire in shielding gases from pipes of K56 steel grade from various manufacturers, with wall thickness of 12.0 mm and diameter of 1220 mm.

During welding, a thermal cycle was recorded, which made it possible to determine the absolute heating temperature and calculate the cooling rate of the metal in various zones of the welded joint using the procedure from [9].

Samples for testing were cut from the manufactured circular welded joints, according to the configuration shown in Figure 3. The weld seam reinforcement on the samples was removed, and a surface semi-elliptical crack-like stress concentrator was applied along the welded joint with a length of 36 mm, a depth of 4 mm, and a width of 0.2 mm. Concentrator application areas:

s = 0 mm - fusion line (FL);

s = 2 mm from the fusion line (FL+2); - s = 5 mm from the fusion line (FL+5).

If the condition is met $B \geq 6t$, uniaxial tension of this specimen configuration makes it possible to realize a stressed-deformed state in its central part across the width, similar to that which arises in a pipeline when it is loaded with internal pressure [10]. A total of 72 samples were made.

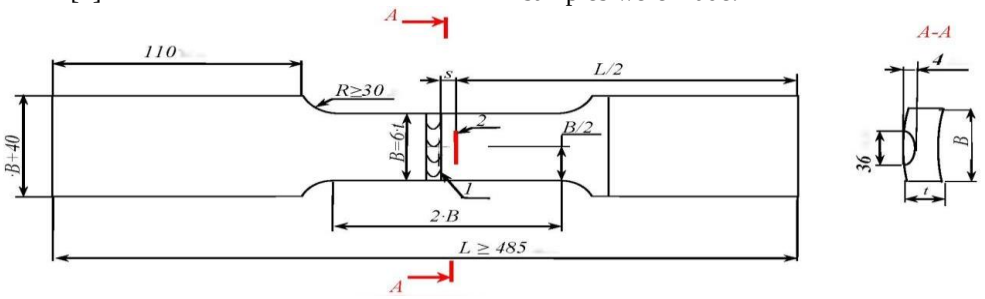

1 – welded seam; 2 – stress concentrator

Figure 3 – Configuration of segmental specimens

The sample testing program provided for their cyclic loading on the basis of 10^5 cycles (or till destruction).

Loading parameters consisted of two stages: The maximum load in the cycle is 0.9 · σt. Cycle ratio is R = 0.1. Duration of loading is 10^4 cycles.

The maximum load in the cycle is 0.45 · σt. Cycle ratio is R = 0.1. Duration of loading is $5 \cdot 10^3$ cycles.

The implementation of the above loading parameters was carried out in turn, during the entire number of cycles (or till destruction). This approach makes it possible to obtain different fracture roughness at stages 1 and 2 of loading, as a result of different rates of crack growth, which makes it possible to determine the kinetics of its development [11].

Also, as in the case of testing samples with the structure shown in Figure 2, upon completion of the model tests, CCGR were built, from which the parameters of crack resistance K_{Ic}, C and n were determined. Taking into account the loading scheme of the samples and the parameters of the applied crack-like concentrators, the expression from API 579/ASME FFS-1 was used to calculate the KI,[6]:

$$K_I = \sigma_\Phi \frac{\sqrt{\pi \cdot H}}{\Phi} \cdot F_{tr} \qquad (2)$$

where $\Phi = \sqrt{1{,}0 + 1{,}464 \cdot \left(\frac{H}{a}\right)^{1{,}65}}$

$$F_{тр} = M_1 + M_2 \cdot \left(\frac{H}{\delta}\right)^2 + M_3 \cdot \left(\frac{H}{\delta}\right)^4$$

$$M_1 = 1{,}13 - 0{,}09H/\text{a}$$

$$M_2 = -0{,}54 + \frac{0{,}89}{0{,}2 + H/a}$$

$$M_3 = 0{,}5 - \frac{1}{0{,}65 + H/a} + 14(1 - H/a)^{2{,}4}$$

[6] API 579/ASME FFS-1 Fitness For Service. Fitness For Service (American Society of Mechanical Engineers, ASME, 2007), USA

σ_f is nominal stress perpendicular to the plane of the crack at the point at which the defect is located, MPa; *H* is the depth of the calculated crack, mm; a is half-length of the calculated crack, mm.

At the second stage, the determined empirical correlations were checked.

For this purpose, circular welded joints of pipes and butt welded joints of sheets of the tank wall were made using welding technologies approved for use in the Transneft PJSC (see Table 3).

Table 3

The scope of welded joints prepared for testing at the second stage

Item No.	Welding technology	Pipe diameter, mm	Sheet size (length x width), mm	Number of welded joints, pcs.
Circular welded pipe joints				
1	MMA*	720-1220	-	12 (3 welded joints each for four different pipe manufacturers)
2	MMA+FCAW-S*	720-1220	-	12 (3 welded joints each for four different pipe manufacturers)
3	MWSG-AG+AWFCW-AG*	720-1220	-	12 (3 welded joints each for four different pipe manufacturers)
4	AWSG-AG*	720-1220	-	12 (3 welded joints each for four different pipe manufacturers)
5	MMA+ASMAW*	720-1220	-	12 (3 welded joints each for four different pipe manufacturers)
Butt welded joints of the tank wall sheets				
6	MMA*	-	1500x300	6
7	MWSG-AG*	-		6
8	AWFCW-AG*	-		6
9	MWSG-AG+ASMAW*	-		6

* MMA – manual metal-arc welding with a basic coated stick electrode ; FCAW-S - fluxcored automated welding - self-shielded filler wire; MWSG-AG - mechanized welding with solid wire in active gases and mixtures; AWFCW-AG - automatic flux-cored wire welding in active gases and mixtures; AWSG-AG - automatic welding with solid wire in active gases and mixtures; ASMAW - automatic submerged-arc welding.

Samples were cut from the welded coils and sheets for research and testing of various zones of the welded joint (weld metal, fusion line, sections of the weldaffected zone), similar to those shown in Table 2.

Results

Processing the results of laboratory tests and metallographical observations of thermally treated templates made it possible to build an empirical diagram reflecting the relative change in the basic mechanical properties of the metal as the rate of its cooling increases (Figure 4). The determined correlation is also associated with structural changes occurring in the metal, caused by the action of the thermal cycle (see Figure 4).

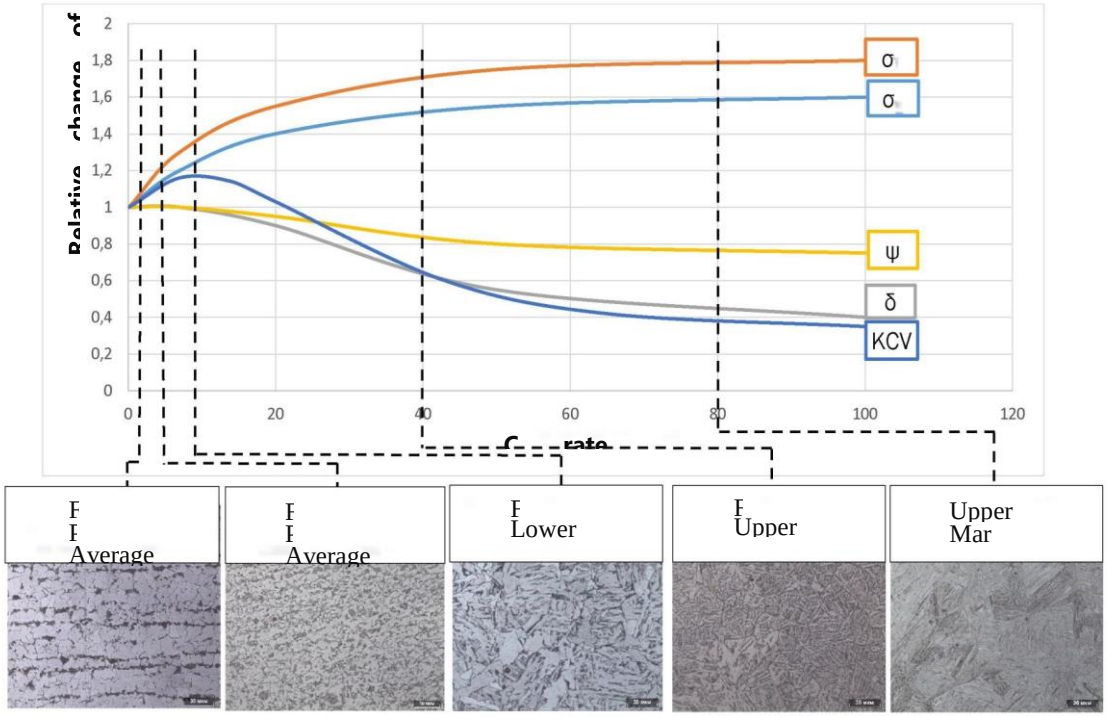

Figure 4 – Influence of the metal cooling rate in the Ac1-Ac3 temperature range on its basic mechanical properties

9

The correlation shown in Figure 4 turned out to be little sensitive to the maximum heating temperature (900 and 1100 °C), and therefore it can be accepted as universal for all cases of metal heating above the Ac3 temperature. When the metal is heated to a temperature below Ac3, the quantitative effect of the cooling rate on the basic mechanical properties of the metal can be corrected by the correction factor *K*:

$$K = 1 - \frac{TAc3 - Tmax}{TAc3 - TAc1}, \; at \; TAc1 \leq Tmax \leq TAc3 \quad (3)$$

$$K = 0, \; at \; T_{max} < T_{Ac1}$$

where T_{Ac1}, T_{Ac3} are, respectively, the temperatures of the beginning and end of phase transformations in the metal, °C; T_{max} is a maximum heating temperature during welding, °C.

From the data presented in Figure 4, it can be seen that the basic mechanical properties are determined by the structural state of the metal.

At a cooling rate in the range of 0.5 - 6 ºC/sec, the metal is characterized by a ferrite-pearlite structure, the σt - yield strength; σv - tensile strength; δ - percentage of elongation; ψ - contraction ratio; KCV - impact toughness

average score of which increases from 9 to 11 according to GOST 5639-826, as the cooling rate increases. Based on the change in properties in the above range, the following expressions were obtained, reflecting the effect of the average grain size of the ferrite-pearlite matrix:

on the values of impact toughness KCV:

$$K_{KCV} = 0{,}1\Delta N + 1 \quad (4)$$

on the values of tensile elongation δ and ultimate tensile strength δ and yield value σ_v:

$$K_{\sigma v} = K_{\delta} = 0{,}05\Delta N + 1 \quad (5)$$

where K_{KCV},K_{KCV}, $K_{\sigma v}$, K_{KCV}, $K_{\sigma v}$, K_{δ} is respectively, the correction coefficients of the values of impact toughness, ultimate strength and percentage of elongation, depending on the value of the average grain grade of the ferrite-pearlite matrix; K_{KCV}, $K_{\sigma v}$, K_{δ} – respectively correction coefficients of values of impact toughness, tensile strength and relative elongation, depending on the value of the average grain score of the ferrite-pearlite matrix; ΔN is a change in the value of the average grain grade of the ferrite-pearlite matrix according to GOST 5639-826, relative to the initial state (for which the mechanical properties are known).

No effect of grain size on the values of properties such as yield strength σ_t and tensile constriction σ_t and tensile contraction ratio ψ was found.

Beginning with a cooling rate of 10 ºC/sec, a bainite structure was formed in the metal. Moreover, at lower cooling rates (about 10 °C/sec), the lower bainite with its characteristic laminar morphology was

identified [12-14], and at higher cooling rates (about 40 ° C/sec), the upper bainite with a plumose structure [12-14] (see Figure 4).

The bainite morphology had a very noticeable effect on the properties of the metal. Thus, during cooling at a rate of 10 ºC/sec, increased strength and stable plastic characteristics of the metal were recorded, which ensured the highest values of its impact toughness. Upon cooling at a rate of 40 ºC/sec, a further increase in strength characteristics and a significant metal ductility dip in both the plasticity of the metal and the values of its impact toughness were observed.

Since no other structural changes were observed in the considered range of cooling rates (in particular, the appearance of quenching structures), the results obtained were used to determine the quantitative effect of the bainite structure on the mechanical properties of the welded joint (Table 4). Moreover, in this case, it is advisable to determine the effect of bainite irrespective of its exact amount, but only upon actual detection (depending on morphology).

Table 4

Influence of the bainitic structure of the metal on the properties of the welded joint

Structure name	Influence on metal properties				
	Tensile strength σ_v	Yield strength σ_t	Percentage of elongation δ	Contraction ratio ψ	Impact toughness KCV
Upper bainite (plumose)	+15%	+15%	-15%	-10%	-25%
Lower bainite (laminar)	+10%	+10%	0%	0%	+15%

Similarly, the influence of the quenching structure (martensite) in the metal detected at cooling rates of about 60-80 °C/sec was being determined (see Figure 4), presented in Table 5.

Table 5

Influence of the martensitic structure of the metal on the properties of the welded joint

Structure name	Influence on metal properties				
	Tensile strength σ_v	Yield strength σ_t	Percentage of elongation δ	Contraction ratio ψ	Impact toughness KCV
Martensite	+40%	+50%	-50%	-25%	-60%

Tests for the cyclic crack resistance of specimens with the structure shown in Figure 2 made it possible to obtain the correlation between the values of the parameters K_{Ic},, C and n with the metal cooling rate (Figure 5).

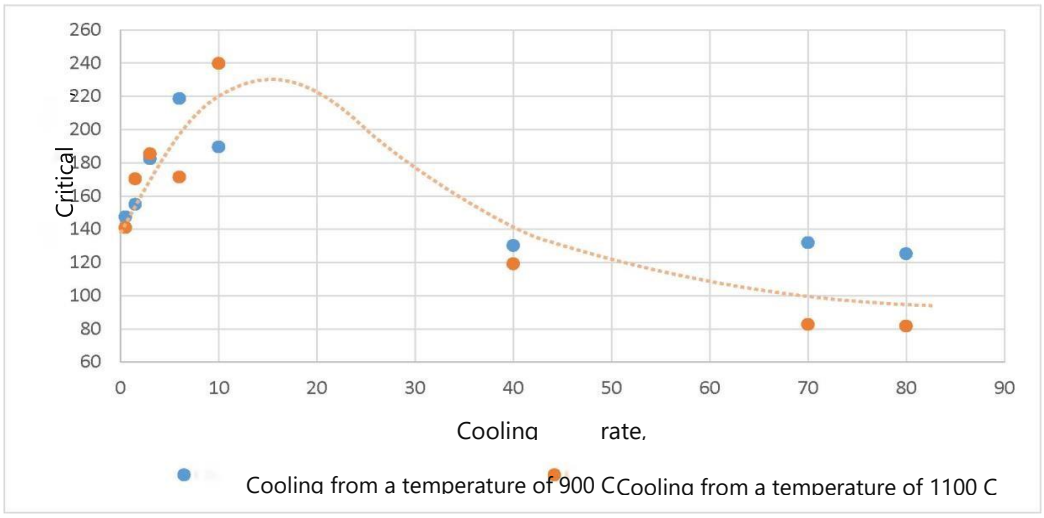

a

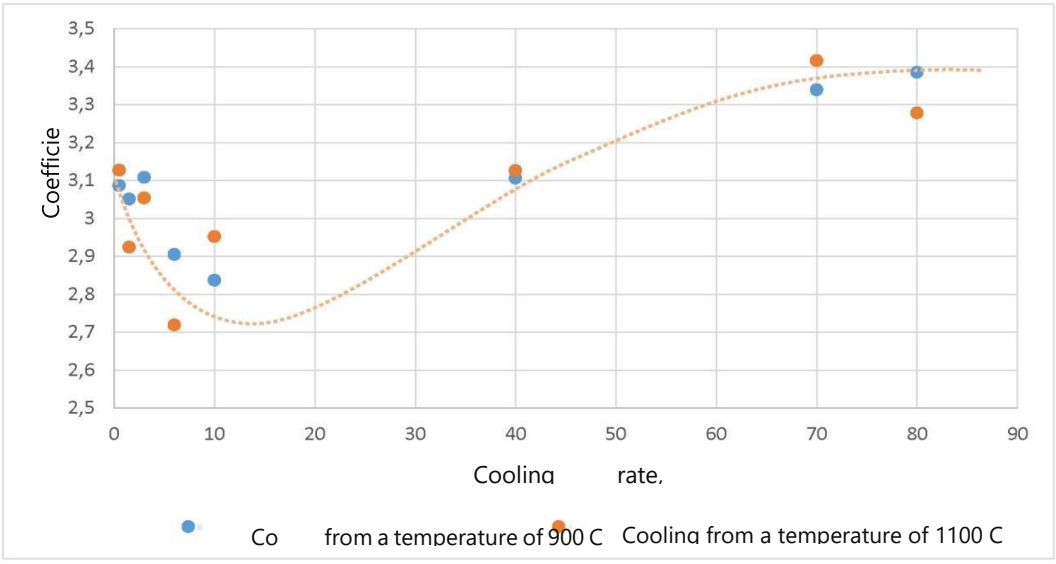

b

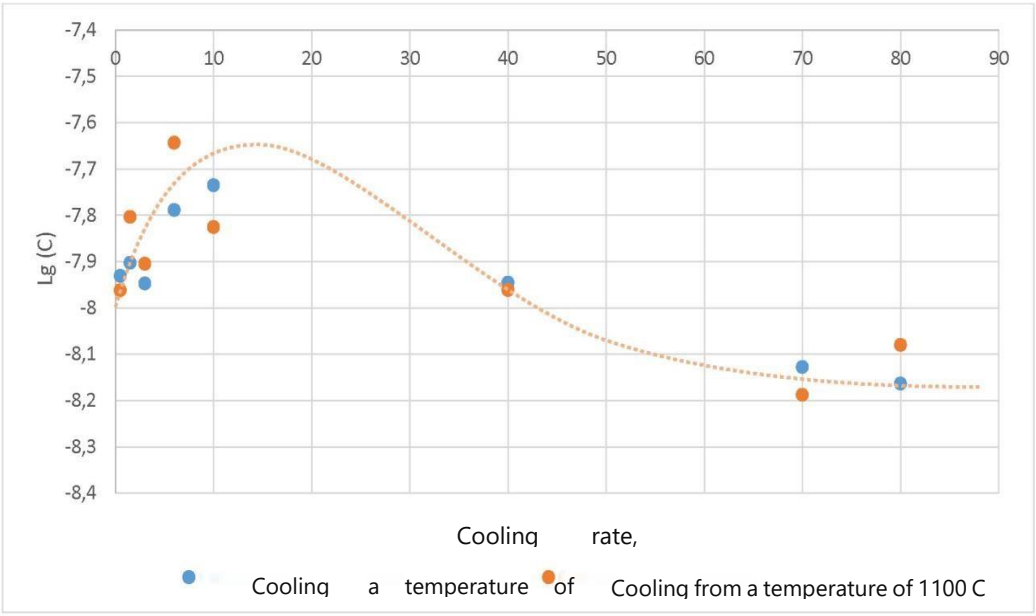

c

Figure 5 – Dependence of crack resistance parameters on the metal cooling rate a – for K_{Ic}; b – for n; c – for C

The reliability and universality of the data obtained was being assessed by comparing them with the test results of segment specimens with the structure shown in Figure 3. The values obtained at cooling rates close to those that occurred in the FL zones, FL + 2 and FL + 5 when welding the coils were being compared (Table 6).

Table 6 shows that the spread of the parameters of crack resistance of the metal of two structures of specimens with different types of stress concentrators is small. The greatest differences are observed in the average K_{Ic} values at a cooling rate characteristic of the FL zone, which can be explained by the difference in the chemical composition (in segmented specimens in this zone, the chemical composition is also affected by the welding consumables). In other cases, the crack resistance parameters are similar. This result demonstrates that the use of a compact specimen structure for testing (see Figure 2) allows us to obtain reliable parameters of metal crack resistance.

Comparing the diagrams from Figures 4 and 5, it can be seen that the change in the parameters of crack resistance is associated with a change in the basic mechanical properties: high impact toughness and plasticity of the metal correspond to high values of crack resistance parameters and vice versa.

Table 6

Average values of crack resistance parameters of two types of specimens at similar cooling rates

Crack resistance parameter	**Average value for specimens in Figure 3**	**Average value for specimens in Figure 2**	**Error**
	Concentrator application area: FL	**Heat treatment conditions No. 2 from the Table 1**	
K_{Ic}	126.74	170.31	-25.6%
Lg(C)	-7.95	-7.80	-1.9%
n	3.107	2.924	+6.2%
	Concentrator application area: FL+2	**Heat treatment conditions No. 3 from the Table 1**	
K_{Ic}	172.11	185.36	-7.15%
Lg(C)	-7.92	-7.91	+0.1%
n	3.071	3.054	+0.1%
	Concentrator application area: FL+5	**Heat treatment conditions No. 11 from the Table 1**	
K_{Ic}	160.42	182.33	-12.01%
Lg(C)	-7.88	-7.95	-0.9%
n	3.018	3.108	-2.9%

Based on this pattern, an attempt was made to obtain an empirical expression linking these characteristics.

The analysis showed that the key basic properties that should be used to achieve this goal are tensile elongation δ, impact strength KCV_{-20} and the ratio of yield strength to ultimate tensile strength σ_t/σ_v. The KCV values obtained at a temperature of -20 °C are used due to their greater sensitivity to changes in the metal. Moreover, in order to achieve the best correlation between the above properties and the crack resistance parameters K_{Ic}, C and n, the former should be considered together, through the proposed "complex coefficient of metal durability" K_{Σ}, calculated as:

$$K_{\Sigma} = \frac{27{,}5(1 - e^{-\frac{\delta}{0{,}225}}) \cdot 0{,}11(KCV_{-20})}{2{,}37e^{1{,}74(\sigma_t/\sigma_v)}} \quad (6)$$

In this case, the relationship between the values of the complex coefficient of metal durability K_{Σ} and the crack resistance parameters K_{Ic}, C and n has the form shown in Figure 6, and can be described by the expressions:

$$K_{Ic} = 40{,}793K_{\Sigma}^{0{,}313} \quad (7)$$

$$n = -0{,}194\ln(K_\Sigma) + 3{,}957 \quad (8)$$

$$Lg(C) = 0{,}0029K_\Sigma - 8{,}227 \quad (9)$$

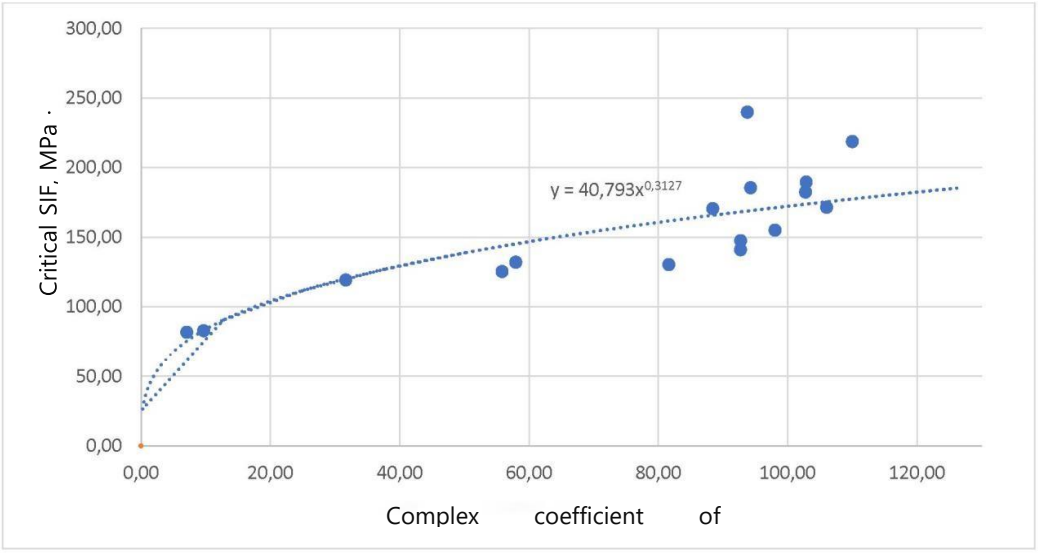

a

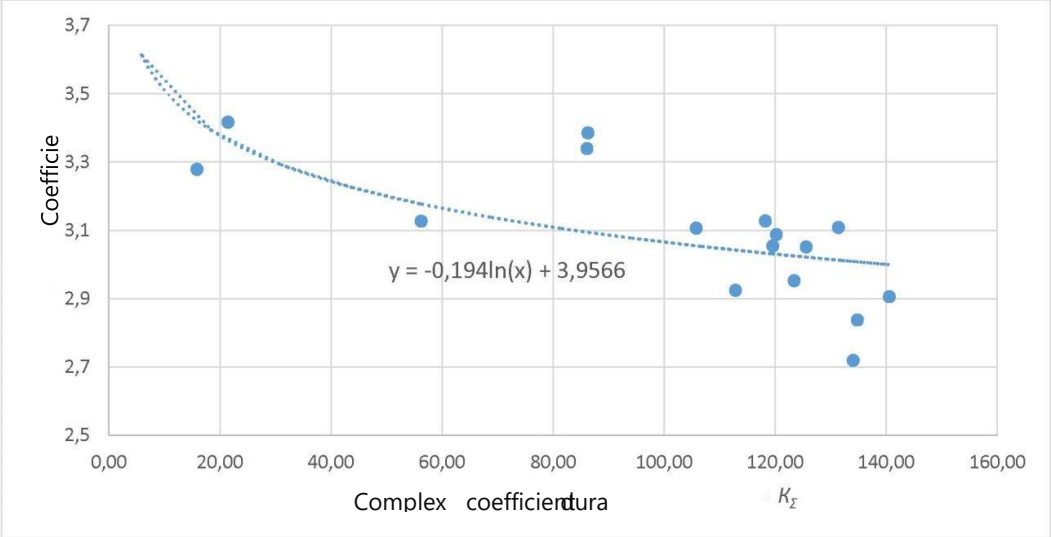

B

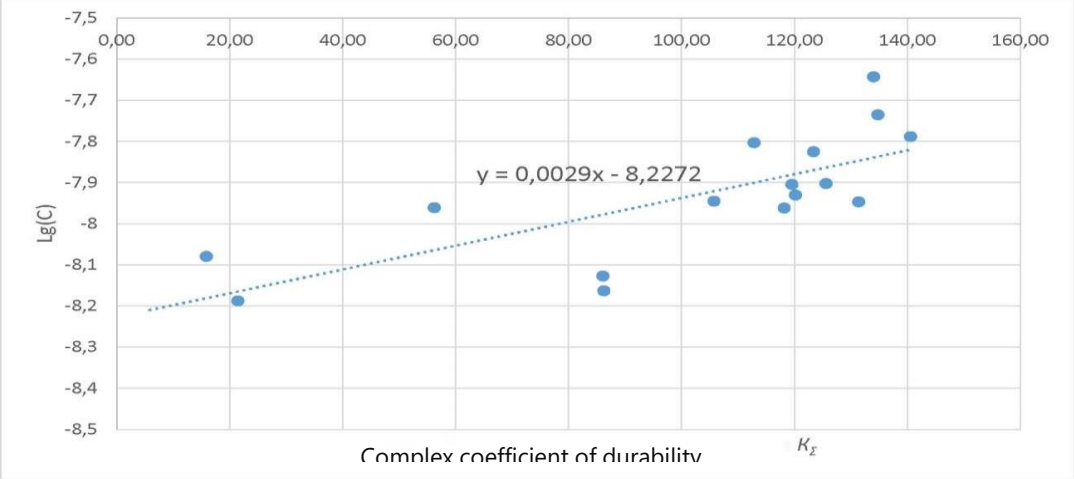

c

Figure 6 – The correlation between the parameters of the crack resistance of the metal and the complex coefficient of metal durability K_Σ

a – dependence of KIc on KΣ; b - dependence of n on KΣ; c - dependence of Lg(C) on KΣ

Thus, the results obtained make it possible to predict its mechanical properties using data from the thermal cycle of welding and/or information on the structural condition of the metal of the welded joint, and from them, the parameters of crack resistance used within the force criterion of fracture mechanics. However, it should be noted that the dependences shown in Figure 4 are valid only for the weld-affected zone with the original ferrite-perlite structure of the base metal. In the case when there is an initial intermediate or quenched structure of the base metal, the data from Tables 4 and 5 can be used, which should be proportionally corrected when the corresponding structure disappears.

For forecasting of the properties of the weld metal using the diagrams from Figure 4, it is necessary to evaluate its initial properties. The values of these properties can be obtained by calculation, based on the chemical composition [15]: *The tensile strength of the welded seam metal, kg/mm²:*

$$\sigma_{vs} = 4.8 + 50C + 25.2Mn + 17.5Si + 23.9Cr + 7.7Ni + 8W + 70Ti \quad (10)$$
$$+ 17.6Cu + 2.9Al + 16.8Mo$$

Yield strength of the welded seam metal, kg/mm²:

$$\sigma_{ts} = 0.73\sigma_{vsh} \quad (11)$$

Percentage of elongation of the welded seam metal, %:

$$\delta_s = 50.4 - (21.8C + 15Mn + 4.9Si + 5.8Cr + 2.4Ni + 2.2W + \quad (12)$$

6.6Ti + 6.2Cu) + 17.1Al + 2.7Mo, *Impact strength of the welded seam metal, kgf * m/cm²:*

$$_{ns} = 23.3 - (25.7C + 6.4Mn + 8.4Si + 2.4Cr + 1.6Ni + 0.5W + \quad (13)$$
$$15.4Ti + 4Cu + 18Al + 1.4Mo),$$

The validity of relations (10) – (13) was confirmed at the concentration of chemical elements in accordance with Table 7.

Table 7

The content of chemical elements in steel, at which relations (10) – (13) are valid

C	Si	Mn	Cr	Ni	Mo	Cu	Al	Ti	W
≤ 0.3%	≤ 1.0%	≤ 2.5%	≤ 3.0%	≤ 3.0%	≤ 1.0%	≤ 3.0%	≤ 0.75%	≤ 0.35%	≤ 2.0%

Determination of the chemical composition of the welded seam metal can be performed both by direct measurements and analytically, using the expression [16]:

$$[C]_s = [C]_o + [C]_e(1 - \gamma) \quad (14)$$

where $[C]_s$ is a mass fraction of the element in the welded seam metal, wt. %; $[C]_s$ – mass fraction of the element in the weld metal, mass. %; $[C]_e$ is a mass fraction of the element in the filler metal, wt. %; $[C]_s$ – mass fraction of the element in the weld metal, mass. %; $[C]_e$ - mass fraction of an element in the filler metal, mass. %; $[C]_o$ is a mass fraction of the element in the base metal, wt. %; $[C]_s$ – mass fraction of the element in the weld metal, mass. %; $[C]_e$ - mass fraction of an element in the filler metal, mass. %; $[C]_o$ - mass fraction of an element in the base metal, mass. %; γ is the share of the base metal in the welded seam metal:

$$\gamma = \frac{Fo}{Fe + F0} \quad (15)$$

F_o, F_o, F_e are the areas occupied, respectively, by the base and filler metal in the welded seam.

The correctness of the correlations and relations presented above was confirmed during tests and studies of welded joints of pipes and tanks (see Table 3). Determination of the mechanical properties of the welded seam metal based on its chemical composition and data on the thermal cycle of welding gave the following root-mean-square error:

tensile strength σ_v is 7%;

yield strength σ_t is 12%;

impact strength KCV_{-20} is 14%;

tensile elongation δ is 7%.

Cyclic tests made it possible to confirm the relation of the complex coefficient of metal durability K_Σ with the metal fatigue crack life (Figure 7).

Conclusions

Based on the results obtained, various levels of initial data can be distinguished, which make it possible

to predict the durability of the welded joint with varying degrees of accuracy. At the same time, the more informative the level of the initial data is, the lower the assurance factor established at the calculations can be. The composition of the initial data levels, the procedure for their application and the proposed values of the coefficients correcting the assurance factor used when performing calculations for the strength and durability of welded joints of oil pipelines are shown in Table 8.

Table 8 shows that the most informative level of initial data is the one that includes information about the structural features of the welded joint. The reason for this is that the characteristics included in this level (actual chemical composition and actual structural features of the metal) can be determined during the operation of a particular welded joint using non-destructive testing. As a result, the durability of the welded joint predicted on the basis of the indicated data will be more reliable than in the case of using for this purpose the mechanical characteristics obtained on similar welded joints that have their own welding characteristics and operating history.

It should be noted that during the development of the presented model, factors such as the content of non-metallic inclusions; the course of diffusion processes (separation of the carbide network along grain boundaries, structures breakdown); residual welding stresses; embrittlement (including microcracking) were not taken into account.

Therefore, a separate direction of the development of the presented model, in addition to its further verification, will be the detection of the influence of these factors on the durability of welded joints, as well as the creation of techniques, technologies and approaches that allow to assess (quantitatively or qualitatively) their presence in each analyzed case.

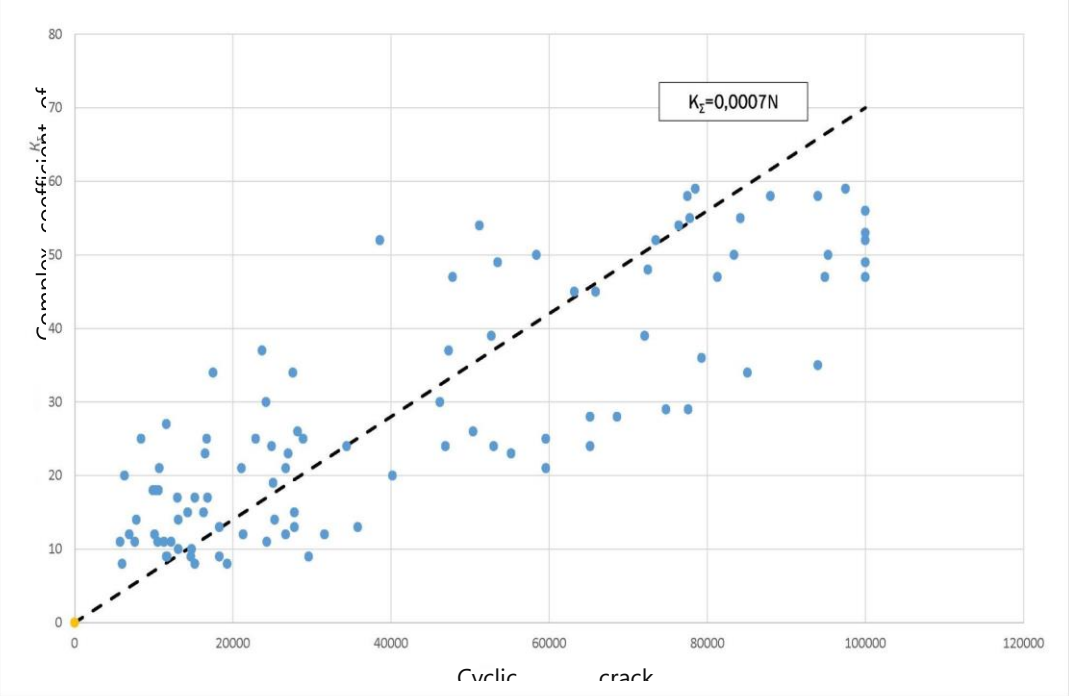

Figure 7 – Correlation between the values of the cyclic crack resistance of different zones of the welded joint and the complex coefficient of metal durability K_Σ (for circular welded joints of pipes)

Table 8

Data levels on the welded joint of the oil pipeline used to predict its durability

No. pos.	Data level	Content of initial data	Adjustment factor value	Sequence of actions when specifying mechanical characteristics
1	Level 1	Certification chemical composition of steel; Certification properties of steel; Welding conditions; Certification chemical composition of welding consumables.	K = 1.00	Calculation of the chemical composition of the metal in accordance with expressions (14) – (15) *. Calculation of the basic properties of the metal in accordance with the expressions (10) – (13)**. Correction of the basic properties of the metal, taking into account the thermal cycle of welding in accordance with Figure 4. Forecasting of metal crack resistance characteristics in accordance with expressions (6) – (9).

2	Level 2	Basic mechanical characteristics of the welded joint.	K = 0.95	1. Forecasting of metal crack resistance characteristics in accordance with expressions (6) – (9).
3	Level 3	Basic mechanical characteristics of the welded joint. Characteristics of static and cyclic crack resistance.	K = 0.95 when calculating the load-bearing capacity K = 0.92 when calculating crack resistance	Clarification of mechanical characteristics is not required
4	Level 4	Actual parameters of the welded joint metal structure; Actual chemical composition of the metal of the welded joint.	K = 0.87	Calculation of the basic properties of the metal in accordance with the expressions (10) – (13)**. Correction of the basic properties of the metal in accordance with Tables 4 and 5 (and expressions (4) – (5) for the metal of the weld-affected zone). Forecasting of metal crack resistance characteristics in accordance with expressions (6) – (9).

* Applicable for welded seam metal. For the weld-affected zone, the chemical composition of the metal is taken to the corresponding certification values for the base metal.

** Applicable for welded seam metal. For the weld-affected zone, the basic properties are assumed to correspond to the certification values for the base metal.

References

Idrisov, R.Kh. Analysis of the accident rate of the main pipelines of Russia / R.Kh. Idrisov, K.R. Idrisova, D.S. Kormakova // Transport and storage of petroleum products and hydrocarbon raw materials. - 2019. - No. 2. - pp. 44-46.

Aladinsky, V.V. Formation of requirements for the geometry and properties of welded joints of pipes, ensuring the reliability of pipelines / V.V. Aladinsky, A.V. Melnikova // Science and technology in the gas industry. - 2009. - No. 4 (40). - pp. 43-48.

Golikov, N.I. Strength of welded joints of tanks and pipelines operating in the conditions of the North / N.I. Golikov, A.P. Ammosov. - Yakutsk: Publishing house of the North-Eastern Federal University, 2012. - 232 pages.

Makarov, E.L. Theory of weldability of steels and alloys / E.L. Makarov, B.F. Yakushin. - M .: Publishing house of the Moscow State Technical University named after N. E. Bauman, 2014, 487 pages.

Savkin, A.N. Methods for determining the coefficients of the equation for the growth rate of a crack under cyclic loading / A.N. Savkin, A.V. Andronik, R. Koraddi // Factory laboratory. Diagnostics of materials.- 2016.- Volume 82.- No. 1.- pp. 57-63.

Mamontov, V.A. Construction of a diagram of fatigue destruction of ship shaft models / V.A. Mamontov, T.A. Kuzhakhmetov, R.U. Iksanov, Doan Van Tin // Bulletin of ASTU.- 2008.- No. 5 (46) .- pp.44-49.

Stress Intensity Factors Handbook: In 2 volumes. Volume 1: Translated from English/ Eds. Yu. Murakami. - M .: Mir, 1990.- 448 pages.

Terentyev, V.F. Fatigue of metallic materials / V.F. Terentyev.– M.: Nauka, 2003.– 254 pages.

Zorin, A.E. Analysis of structural and thermal processes during welding (to optimize the technology of cutting out circular welded joints of pipelines) / A.E. Zorin // Oil, Gas and Business.- 2011.- No. 6.- pp. 67-70.

Zorin, A.E. Development of coupon structure for conducting mechanical tests of metal pipes / A.E. Zorin // The territory of "NEFTEGAZ".- 2015.- No. 3.- pp. 124-128.

Zorin, A.E. Scientific and methodological support of the system for maintaining the operability of long-term operated gas pipelines: dis. ... of DEng: 25.00.19 / Zorin Alexander Evgenievich. - Moscow, 2016. - 332 pages.

Belchenko, G.I. Fundamentals of metallography and plastic deformation of steel / G.I. Belchenko, S.I. Gubenko. - Kiev: Vishcha shkola, 1987. - 240 pages.

Bidulya, P. Steel foundry practice, 1968.- 319 p.

Geller, Yu. Tool steels, 1978.- 659 p.

Ockerblom, N.O. Design of technology for the production of welded structures / N.O. Ockerblom, V.P. Demyantsevich, I.P. Baikova. - Leningrad:

Sudprom GIZ, 1963. - 602 pages.

Welding in machine engineering: Handbook in 4 volumes / Eds. N.A. Olshansky.– M.: Mashinostroenie, 1978.- Vol. 1.- 504 pages.

INFORMATION ABOUT AUTHORS

Full names	Position, place of work
Neganov Dmitry Alexandrovich	D.Eng.Sc., First Deputy General Director Transneft R&D, LLC 8(495)950-8295 add. 2100
Makhutov Nikolay Andreevich	Associate member of the RAS, Chief Researcher, Transneft Research Institute LLC 8(495)950-8295 add. 2650
Zorin Alexander Evgenievich (corresponding author)	D.Eng.Sc., Leading Researcher of the Welding Laboratory of the Welding Department and Tanks of the Steel and Welding, Strength Calculations Center of the Scientific Research Institute Transneft LLC, 8(495)950-8295 add. 4823
Studenov Evgeny Pavlovich	Head of the Steel and Welding, Strength Calculations Center, Scientific Research Institute Transneft LLC, 8(495)950-8295 add. 2830
Kolesnikov Oleg Igorevich	Head of the Welding and Tanks Department of the Steel and Welding, Strength Calculations Center, Scientific Research Institute Transneft LLC, 8(495)950-8295 add. 2880

УДК 621.039 : 539.17

WAYS TO IMPROVE THE HEAT GENERATOR A. ROSSI

Tertyshnik E.G.
Independent researcher, Obninsk Kaluga region
DOI: 10.31618/ESU.2413-9335.2022.1.98.1652

ABSTRACT

Based on the test report of the heat generator by A. Rossi (2011, Lugano), the authors calculated that the summa of nuclear energy had been generated by the heat generator for 30 days exeeded 2900 MJ . To improve the operational characteristics of the device, it is proposed to use a high-frequency generator to heat the reacting mixture. The use of titanium instead of nickel in the heat generator can also be useful. An experiment was carried out in during which a nuclear reaction in a mixture of 5 g of nickel and 0.5 g of lithium aluminum hydride was initiated by heating in a household microwave oven. Gamma analysis of the mixture after it had cooled revealed the presence of a number of short-lived nuclides including ^{46}K (half-life 1.75 min.), ^{91m}Mo (half-life 1.077 min.), ^{168m}Lu (half-life 6.70 min.). At the moment of start of measurements, the activity of these nuclides ranged from 0.5 to 1 Bq.

Key words: low energy nuclear reaction; termogenerator A. Rossi; gamma spectrometry; nickel; titanium; high frequency heating

Introduction. The production of electricity at nuclear power plants and the processing of spent nuclear fuel are associated with the risks of man-made pollution of the environment. Therefore, the problem of searching for sources of environmentally friendly energy and conducting experiments on energy production based on low-temperature nuclear reactions is relevant.The idea of using cold transmutation of atoms (nuclei) to obtain clean and cheap energy was successfully implemented by Italian researchers S. Focardi and A. Rossi and became widely known [1]. At the same time, the achievements of the Russian inventor A.V. Vachaev, who created in 1994 an industrial installation in which a water flow was passed through the region of a high-frequency plasma discharge, and as a result, energy was created and new elements were synthesized at a rate of their formation of the order of kg/min [2], did not attract attention and went unnoticed by the world scientific public. This is probably due to the fact that after the death of A.V. Vachaev in 2000, his employees could not put the unit into operation, while the prototypes of Rossi's heat generator operate in many countries [3].

Analysis of the operation of the Rossi thermogenerator

As reported in [4,5], the heat generator is a ceramic tube, inside which contains a fuel - mixture of 1 g of nickel powder and 0.1 g of lithium aluminum hydride ($LiAlH_4$), with a heating coil wound on its surface. With the help of this spiral, the tube with fuel was heated up to 1260-1400°C. During testing, the amount of energy spent on heating, and the amount of thermal energy generated by the installation. It is indicated that during the 32 days of testing, the E-cat device produced 5800 MJ of heat, which is more than 3 times the energy used for electric heating. The spent fuel was subjected to mass spectrometric analysis, which revealed significant changes in the isotopic composition of the fuel, unambiguously indicating the origin of nuclear energy (Table 1).